

PAPER • OPEN ACCESS

Optimization of on-chip photonic delay lines for telecom wavelengths

To cite this article: A Prokhodtsov *et al* 2018 *J. Phys.: Conf. Ser.* **1124** 051052

View the [article online](#) for updates and enhancements.



IOP | ebooks™

Bringing you innovative digital publishing with leading voices to create your essential collection of books in STEM research.

Start exploring the [collection](#) - download the first chapter of every title for free.

Optimization of on-chip photonic delay lines for telecom wavelengths

**A Prokhodtsov^{1,2}, P An^{2,3}, V Kovalyuk^{2,3}, E Zubkova^{2,3}, A Golikov^{2,4},
A Korneev^{2,4}, S Ferrari^{5,6}, W Pernice^{5,6}, G Goltsman^{1,2,3}**

¹National Research University Higher School of Economics, Moscow 101000, Russia

²Department of Physics, Moscow State Pedagogical University, 119992, Russia

³Zavoisky Physical-Technical Institute of the Russian Academy of Sciences, 420029, Russia

⁴Moscow Institute of Physics and Technology (State University), 141700, Russia

⁵Institute of Physics, University of Münster, 48149, Germany

⁶CeNTech - Center for Nanotechnology, University of Münster, 48149, Germany

Abstract. In this work, we experimentally studied optical delay lines on silicon nitride platform for telecomm wavelength (1550 nm). We modeled the group delay time and fabricated spiral optical delay lines with different waveguide widths and radii as well as measured their transmission. For the half etched rib waveguides we achieved the losses in the range of 3 dB/cm

1. Introduction

Integrated optical delay lines (DL) can be successfully used for time delay in microwave photonics, highly stable microwave generators, in the processing of optical signals as well as in the construction of quantum-photonic integrated circuits (QPICs) [1, 2]. Optical true time delays (OTTD) can also be used for broadband phased array antenna applications to reduce beam distortion due to frequency variation and electromagnetic interference [3]. Different fully-integrated OTTD have been demonstrated [4-6], where the maximum time delay was limited to the picosecond-few nanoseconds range because of high propagation losses. To reduce the overall footprint, usually the delay lines fabricated in the form of a long waveguide are twisted into a spiral. Low-loss (0.08 dB/m) spiral DL have been already demonstrated on silicon chip, and the possibility of realizing 250m long delay line have been discussed [1]. Here we propose as waveguide material low pressure chemical vapor deposited (LPCVD) silicon nitride (Si_3N_4), which is a promising platform for nanophotonic circuits and combines good mechanical properties, low optical absorption in the infrared (IR) and visible wavelength ranges as well as possibility for creation of single-photon sources based on four-wave mixing [7].

2. Device design and modeling

In a planar technology we designed a DL as an Archimedean spiral. The radius of consecutive half-arcs is gradually increased from the center thus forming a spiral. In this realization, the delay line begins with two half-circles, rounding in opposite directions with increasing radius, starting from a minimum value r . Figures 1(a-c) show the single delay line consisting of the spiral path a strait segment and two focusing grating couplers for input and output light. The schematic view of 2D array of delay lines with different waveguide widths $W = 0.9 - 1.3 \mu\text{m}$ (X -axis) and full lengths $l = 1.5 - 40 \text{ mm}$ (Y -axis) is shown in Figure 1(d).



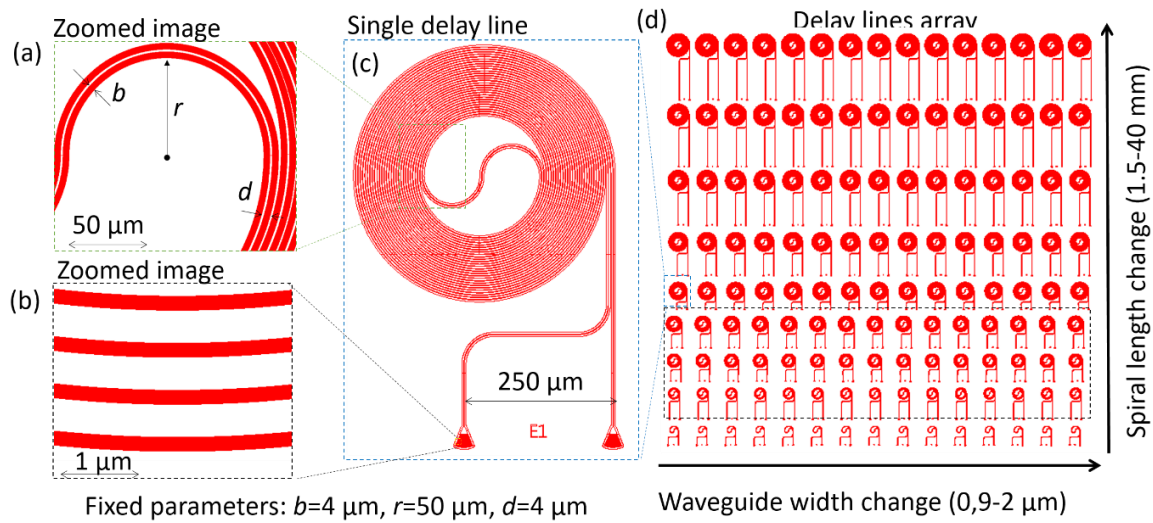


Figure 1. (a-d). Schematic view of a mask layout for e-beam lithography; **(a)** Zoom-in of a central half-circle; **(b)** Zoom-in of a focusing grating coupler; **(c)** Mask layout of a single spiral delay line; **(d)** 2D array of delay lines with different parameters: waveguide width (*X*-axis) and length (*Y*-axis).

The total length of the spiral lines (L_s) was calculated by summing the lengths of the individual clockwise (l_{cw}) and anticlockwise waveguides (l_{aw}):

$$L_s = l_{cw} + l_{aw}. \quad (1)$$

Individual semicircles for each turn form complete circles, adding its length to the first ones placed in the center:

$$L_s = 2\pi r + 2\pi \sum_{k=1}^n R_k, \quad (2)$$

where r is the radius of the smallest arc, k is the coefficient of increase in radius ($k = 1, 2 \dots n$), R_k are the radii of half-arcs. The increment of R_k depends on the separation between the waveguides (d) and a waveguide width (w):

$$R_{k+1} = R_k + \Delta R = R_k + d + w. \quad (3)$$

In most of the cases, there is a need for designing a delay line with a specified and accurate full length. Equation (2) shows that the L_s grows discretely with the number of arcs. In general, the full length can be controlled by the different ways, for example, by the waveguide output angle or by rotating the entire device [8]. In this work, we used the addition straight segments and arcs with a total length L_{SS} calculated as difference between full length L_f and length of the spiral part (L_s):

$$L_{SS} = L_f - L_s. \quad (4)$$

Since the full length increases with the number of half-arcs, we need stop the loop iteration when the length approaches the desired length, while residula length is added to straight segments.

In the first step, we use a numerical calculation of the effective mode index (n_{eff}) in COMSOL Multiphysics. In Figure 3(b) is shown the calculated fundamental quasi-TE mode for a silicon nitride waveguide with a width of $w = 1 \mu\text{m}$ and a half-etched waveguide height of 450 nm plotted for 1550 nm wavelength. Using a dispersion formula for silicon nitride refractive index we calculated $n_{eff}(w)$ for slightly higher and slightly lower wavelength than 1550 nm ($d\lambda_0$) and extracted group refractive index (n_g) using the well-known formula

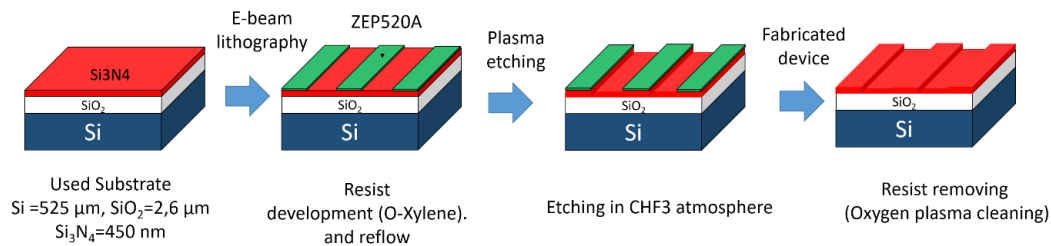


Figure 2. Schematic view of device fabrication rout.

$$n_g = n_{eff} - \lambda_0 \left(\frac{dn_{eff}}{d\lambda_0} \right), \quad (5)$$

After that, we extracted the group delay found the group delay

$$\tau_g = \frac{L_f}{(c/n_g)}, \quad (6)$$

where c is the speed of light.

3. Device fabrication

For the devices fabrication, a multi-layered substrate was used. The thicknesses of silicon (Si), silicon oxide (SiO₂), and silicon nitride (Si₃N₄) were chosen as 450 μm , 2.6 μm , and 450 nm, respectively. The rib waveguides were formed from Si₃N₄ layer by means of one e-beam lithography step with a high-contrast positive resist ZEP 520A. The exposed structures have been developed in O-Xylene for 50 sec and isopropanol has been used as a stopper. Removal of the material below the exposed resist was done by reactive-ion-etching (RIE) in CHF₃ and Ar mixture. The residual resist was cleaned out with oxygen plasma, thus finalizing the fabrication process.

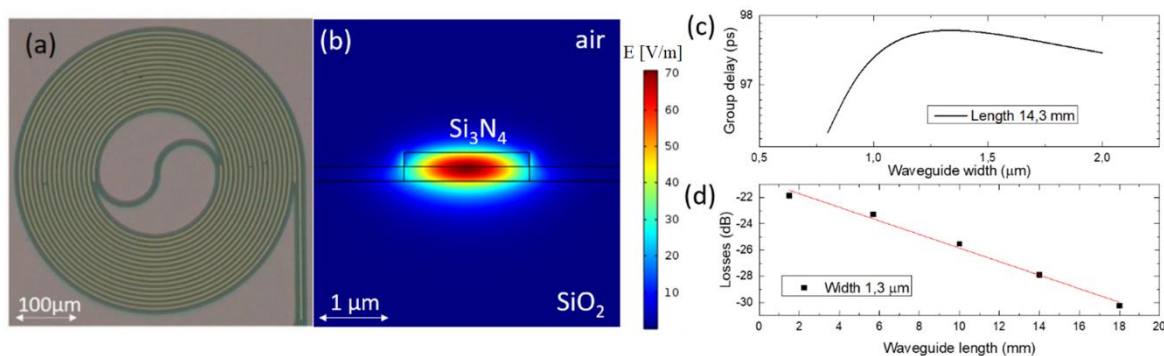


Figure 3. (a-d). (a) Micrograph of the spiral part of DL; (b) The simulation of the quasi TE optical mode, propagated inside the waveguide; (c) Calculated group delay on the waveguide width for DL with the length of 14.3 mm; (d) Losses in spiral waveguide vs waveguide length at fixed waveguide width of 1.3 μm and a minimum radius of $r = 50 \mu\text{m}$.

4. Experimental setup and results

In the second step, we characterized the optical transmission of integrated DLs in the spectral range of 1510 - 1620 nm. We use the experimental setup shown in Figure 4. Light from tunable laser source

(New Focus, TLB 6600) was coupled into the chip using an optical fiber array. Incoming light is adjusted with polarization controller and collected again at the output fiber by a low-noise photodetector and acquired by a PC.

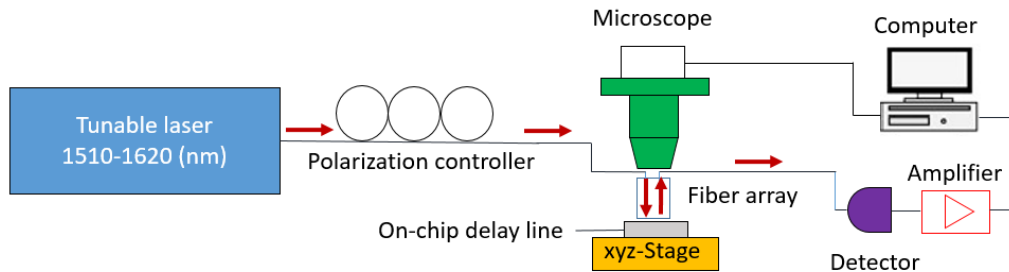


Figure 4. Schematic view of the experimental setup for DLs transmission measurements.

An optical microscope with a USB CMOS camera served to pre-align the device with an fiber array, while a more accurate alignment occurred by adjusting the stage position to maximize the transmitted signal. The dependence of optical losses on the DL length with a minimum radius $r = 50 \mu\text{m}$ is shown in Figure 2(d). Although such a device has a small footprint, due to large losses $\approx 3\text{dB/cm}$, the use in integrated optics is strongly limited and reducing of losses needed.

To reduce the optical losses, we systematically changed both the minimum spiral radius and the width of the waveguide. We found, when the width of the waveguide increases, increases the group delay (due to the increase in the effective refractive index) but the losses are reduced (by removing the maximum of the mode from the edges of the waveguide where the greatest scattering of light occurs).

In the third step, we measured the dependence of the optical losses on minimum spiral radius (Figure 5). Using a minimum radius below $40 \mu\text{m}$ leads to significant optical losses, whereas at large radii they become negligibly small and practically no difference with the losses onto a straight waveguides of the same length can be observed.

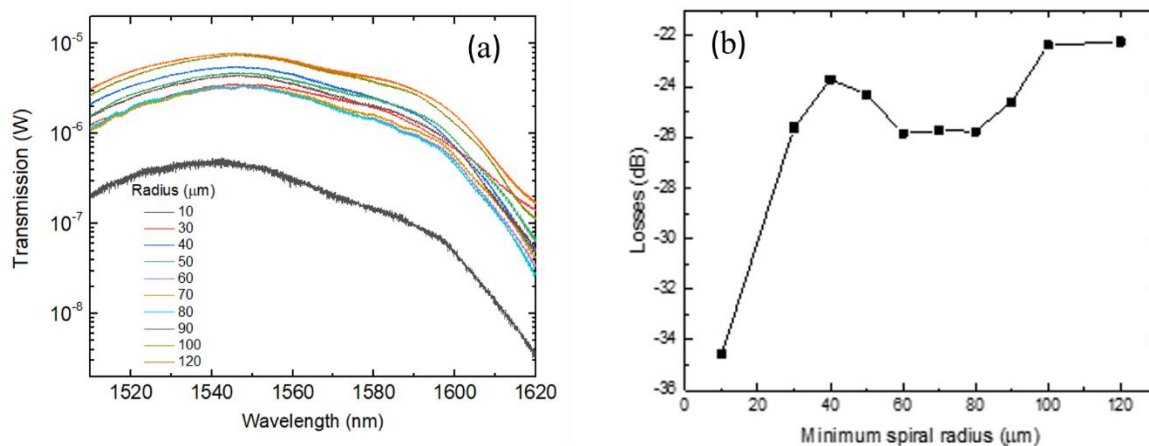


Figure 5. (a, b). (a) The measured transmission spectra of DLs together with focusing grating couplers; (b) Optical losses in spiral waveguide vs minimum spiral radius in a range of 20-120 μm at a fixed waveguide length of 10 mm and waveguide width of $1.4 \mu\text{m}$.

5. Conclusion

We fabricated delay lines with different parameters of the length and width of the waveguide and studied their optical transmission and time delay performance. We found the spiral losses in a range 3 dB/cm as well as simulated the dependence of group delay vs waveguide width in order of 100 ps. Further work will be devoted to the fabrication of delay lines for integrated optical switchers using in spontaneous four-wave-mixing [9], as well as their integration with other integrated optical elements including sources, logic elements and single-photon detectors [10].

Acknowledgments

P. An, V. Kovalyuk, E. Zubkova and G. Goltsman acknowledge support by the Russian Science Foundation (project No. 16-12-00045; device design and testing). A. Prokhodtsov and A. Korneev acknowledge support of the Russian Science Foundation (project No. 17-72-30036; nanophotonic circuits modeling) and W. Pernice acknowledges support by the DFG grants PE 1832/1-1 & PE 1832/1-2 and the Helmholtz society through grant HIRG-0005 (fabrication of nanophotonic circuits).

References

- [1] Lee H, Chen. T, Li J, Painter O, and Vahala K J 2012 *Nat. Commun* **3** 867
- [2] Silveerstone J, Bonneau D, O'Brien J L, Thompson M G 2016 *IEEE J. Sel. Top. Quantum Electron.* **22** 390
- [3] Frigyes I, Seeds A J 1995 *IEEE Transactions on Microwave Theory and Techniques* **43** 2378
- [4] Wang X, Howley B, Chen M, Basile P, and Chen R 2006 *Proc, Integr, Photon. Res. Appl. Nanophoton.* 1
- [5] Sumida D S, Wang S, and Pepper D M 2005 *Proc. CLEO* 734
- [6] Zhuang L, Roeloffzen C G H, Hiedeman R G, Borreman A, Meijerink A, and Etten van W 2007 *IEEE Photonics Technology Let* **19** 1130
- [7] Bogdanov S, Shalaginov M Y, Boltasseva A, and Shalaev V M 2016 *Opt. Mater. Express* **7** 111
- [8] Stopinski S, Malinowski M, Piramidowicz R, Kleijn E, Smit M K, Leijtens X J M 2013 *IEEE Photonics J.* **5** 5
- [9] Ramelow S, Farsi A, Clemmen S, Orquiza D, Luke K, Lipson M, and Gaeta A L 2015 *ArXiv:1508.04358v1*
- [10] Pernice W H P, Schuck C, Minaeva O, Li M, Goltsman G N, Sergienko A V, Tang H X 2012 *Nat. Commun* **3** 1325